

RNA/DNA hybrid duplexes with identical nearest-neighbor base-pairs have identical stability

Naoki Sugimoto*, Misa Katoh, Shu-ichi Nakano, Tatsuo Ohmichi, Muneo Sasaki

Department of Chemistry, Faculty of Science, Konan University, 8-9-1 Okamoto, Higashinada-ku, Kobe 658, Japan

Received 12 September 1994; revised version received 26 September 1994

Abstract Energetic behaviors of eight pairs of RNA/DNA hybrid duplexes with identical nearest neighbors have been investigated by UV melting analysis. In the pairs with identical nearest-neighbor pairs, the melting curve traces at the same strand concentration were very similar. The average difference in stabilization energy of these pairs was 4%, which was about expected within experimental error. These results indicate that the nearest-neighbor model is valid for predicting the stability of RNA/DNA hybrid duplexes as well as RNA/RNA and DNA/DNA duplexes.

Key words: RNA/DNA hybrid; Nearest-neighbor model; Thermodynamic parameter; Melting temperature; Stability prediction; Non-denaturing gel electrophoresis

1. Introduction

RNA/DNA hybrids often play an important role in biological systems such as transcription [1] and reverse-transcription [2]. When the information of the DNA sequence is transcribed into RNA, it is considered that about a 12mer RNA/DNA hybrid is formed while about a 17mer DNA double helix bubble is located in the complex with RNA polymerase [3]. The RNA/DNA hybrids are also important in antisense therapy [4]. For regulation of protein function in this therapy, the protein-coding mRNA is targeted by a chemically synthesized oligonucleotide [5]. Complementary association of an invaded oligodeoxyribonucleotide with the mRNA target site inhibits the formation of the characteristic secondary structure of the RNA and translation into peptide. In a further antisense method, it was reported recently that the activity of a retrovirus, like human immunodeficiency virus (HIV), could be inhibited by cleaving at specific sites of mRNA with a DNA–RNA chimeric hammerhead ribozyme [6]. In such cases it is necessary to quantitatively measure the stability of the hybrid. However, little is known about the thermodynamics of RNA/DNA hybrid formation and the parameters precisely predicting its stability.

Thermodynamic parameters based on the nearest-neighbor model have been determined for stabilities of DNA/DNA and RNA/RNA duplexes [7,8], and were also reported for formation of mismatches, dangling ends, internal loops, bulges, and hairpin loops in RNA [9–14]. The parameters were applied successfully to predict stable secondary structures and active centers of nucleic acids [15–19]. The nearest-neighbor prediction may be considered a useful method to determine the stability of RNA/DNA hybrids. However, if the parameters are applied to the prediction of stability of RNA/DNA hybrids, it is very important to know in advance whether the nearest-neighbor model is valid for RNA/DNA duplexes. In this paper,

therefore, thermodynamic behaviors have been investigated for eight pairs of RNA/DNA hybrid duplexes (16 hybrids) with identical nearest neighbors but different sequences. The thermodynamic values have also been obtained for two pairs of RNA/DNA hybrid duplexes (four hybrids) with identical sequences between RNA and DNA strands but different nearest neighbors. Comparison of these results provides a direct test of the nearest-neighbor model for RNA/DNA hybrids.

2. Materials and methods

2.1. Materials

19 ribonucleotides and 19 deoxyribonucleotides were synthesized chemically on a solid support using phosphoramidite procedures and purified with HPLC after deblocking operations. These 38 oligomers were further purified and desalted with a C-18 Sep-Pak cartridge column. Final purity of the oligomers was confirmed by HPLC and was greater than at least 98%. The length of the examined hybrid strands was at least 6 nucleotides consisting of five nearest-neighbor base-pairs and one initiation factor, and at most 12 nucleotides possessing 11 nearest-neighbor base-pairs and an initiation factor.

All experiments were conducted in a buffer containing 1 M NaCl, 10 mM Na₂HPO₄, 1 mM Na₂EDTA, pH 7.0. Single-strand concentrations of the oligonucleotides were determined by measuring the absorbance at 260 nm at a high temperature as described previously [9]. Single-strand extinction coefficients were calculated from mononucleotide and dinucleotide data by using a nearest-neighbor approximation [20]. RNA strand and its complementary DNA strand were mixed with the concentration ratio of 1:1 to obtain each RNA/DNA hybrid.

2.2. CD measurements

CD spectra were obtained on a JASCO J-600 spectropolarimeter equipped with the temperature controller and interfaced to a NEC PC-9801 computer. The experimental temperature was 5.0 °C. The cuvette-holding chamber was flushed with a constant stream of dry N₂ gas to avoid water condensation on the cuvette exterior. All CD spectra were measured from 350 nm to 200 nm in 0.1 cm path length cuvette. The concentration of the samples were 70 μM in 1 M NaCl-phosphate buffer.

2.3. Non-denaturing gel electrophoresis

Electrophoresis experiments were conducted in gels containing 20% polyacrylamide (19% acrylamide, 1% bisacrylamide) with a Atto AEP-500 apparatus cooled with circulating water to provide a running temperature of 5.0 ± 0.5°C. The hybrid samples were diluted into 5 μl buffer containing 10 mM MOPS, 1 mM Na₂EDTA, 1 M NaCl. The solutions were heated to 90°C for 2 min, cooled slowly, incubated at 5.0°C for 24 h, and run at 5.0°C in 1 × TBE buffer (0.09 M Tris, 0.09 M

*Corresponding author. Fax: (81) (78) 435-2539.

Abbreviations: CD, circular dichroism; UV, ultraviolet; HPLC, high-performance liquid chromatography; T_m , melting temperature; MOPS, 3-(*N*-morpholino)propanesulfonic acid; Na₂EDTA, disodium ethylenediaminetetraacetate; Tris, tris(hydroxymethyl)aminomethane.

boric acid, and 0.2 mM EDTA, pH 8.3) for 3 h. Gels were stained in 0.5 $\mu\text{g}/\text{ml}$ ethidium bromide solution. The pictures of gel were taken with Fuji instant black and white film FP-3000 B.

2.4. UV measurements

Absorbance measurements in the UV region were made on a Hitachi U-3200 or U-3210 spectrophotometer. Melting curves (absorbance vs. temperature curves) were measured at 260 nm with these spectrophotometers connected to an Hitachi SPR-7 or SPR-10 thermoprogammer. The heating rate was 0.5 or 1.0°C per min. The water condensation on the cuvette exterior at the low temperature range was avoided by flushing with a constant stream of dry N_2 gas.

The melting curves of all the hybrids at several strand concentrations showed normal melting behaviors, like DNA/DNA and RNA/RNA double helices [15,21]. Melting data were collected and fitted with a NEC PC-9801 computer. The melting temperatures were obtained with the curve fitting procedure described previously [22]. The thermodynamic parameters (ΔH° , ΔS° and ΔG°) for hybrid formation were determined by the van't Hoff method and analyzed as described in section 3.

2.5. Calculation with nearest-neighbor parameters

According to the nearest-neighbor model, a free energy change (ΔG°_{37}) of the non-self-complementary double-helix formation consists of two terms: (i) a free energy change for helix initiation to form a first base-pair in the double helix, and (ii) a free energy change for helix propagation which is the sum of each subsequent base-pair [23]. In a free energy change for helix propagation there are 16 nearest-neighbor sequences for RNA/DNA hybrids, while there are only ten nearest-neighbor pairs for RNA/RNA or DNA/DNA double helices. With the nearest-neighbor parameters about RNA/RNA and RNA/DNA duplexes as reported previously [3,8], the ΔG°_{37} values of the RNA/DNA duplex formation were calculated as the sum of helix initiation and propagation.

3. Results and discussion

3.1. Structure of RNA/DNA hybrid duplexes

It is well known that the CD spectrum of the DNA/DNA double helix has a positive peak around 280 nm and an intense negative peak around 250 nm in the wavelength range from 220 to 350 nm. It means that the structure is a typical B-form conformation. On the other hand, the CD spectrum of RNA/RNA double helix has one positive peak around 270 nm and a relatively weak and a negative peak around 230 nm in the

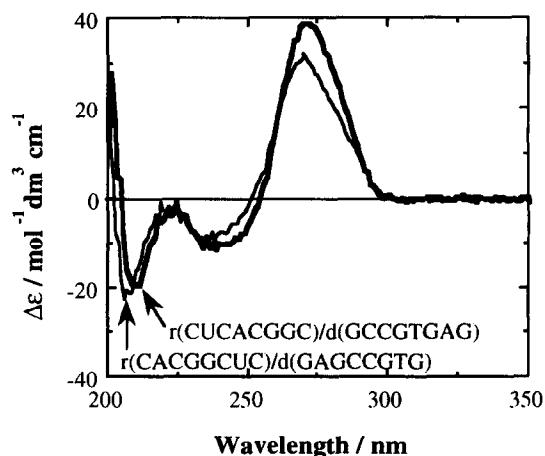


Fig. 1. CD spectra of r(CACGGCUC)/d(GAGCCGTG) (thin line), and r(CUCACGGC)/d(GCCGTGAG) (thick line). The concentration of the samples was 70 μM and measurements were done in 1 M NaCl-phosphate buffer at 5.0°C.

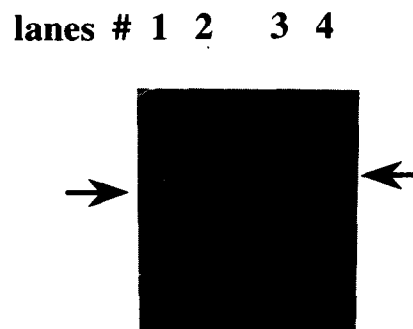


Fig. 2. Electrophoresis of RNA/DNA duplexes in non-denaturing polyacrylamide gels. Lanes 1–4 show the mobilities of r(CACGGCUC)/d(GAGCCGTG), r(CUCACGGC)/d(GCCGTGAG), r(CAGCCGUG)/d(CACGGCTC), and r(GCCGUGAG)/d(CTCACGGC) duplexes, respectively. The gel was run at 5.0°C in 1 × TBE buffer for 3 h.

same wavelength range as DNA/DNA, indicating a normal A-form structure [24].

Fig. 1 shows the CD spectra of r(CACGGCUC)/d(GAGCCGTG) and r(CUCACGGC)/d(GCCGTGAG) hybrid duplexes at 5.0°C. This pair of RNA/DNA hybrid duplexes consists of identical nearest neighbors:

$$\begin{aligned} r(\text{CACGGCUC})/d(\text{GAGCCGTG}) &= r\text{CA}/d\text{TG} + r\text{AC}/d\text{GT} + r\text{CG}/d\text{CG} + r\text{GG}/d\text{CC} + r\text{GC}/d\text{GC} + r\text{C U}/d\text{AG} + r\text{UC}/d\text{GA} \\ &= r(\text{CUCACGGC})/d(\text{GCCGTGAG}) \end{aligned}$$

The spectra of both hybrids with identical nearest neighbors in Fig. 1 have similar shapes: they have an intense positive peak around 270 nm and a small negative peak around 235 nm, although the intensities of the peak at 270 nm are slightly different. The same tendency was found in the other pairs of RNA/DNA hybrids used in the UV melting experiments. This suggests that the RNA/DNA hybrids with identical nearest neighbors have a similar structure which is closer to the A-form conformation than the B-form.

The conformational similarity of the hybrid duplexes was also monitored by polyacrylamide gel-electrophoresis under non-denaturing conditions. It is known that the mobility in the gel is sensitive to the conformation of the nucleic acid [25]. Fig. 2 shows that r(CACGGCUC)/d(GAGCCGTG) seems to have almost the same mobility as r(CUCACGGC)/d(GCCGTGAG). This behavior is also found in the case of r(CAGCCGUG)/d(CACGGCTC) and r(GCCGUGAG)/d(CTCACGGC) with identical nearest neighbors. The same mobility of the two duplexes in each pair shows that the duplexes with identical nearest neighbors have a similar conformation, which was suggested by the CD spectra described above.

3.2. Melting behavior of RNA/DNA hybrid duplexes

Typical melting curves of the r(CACGGCUC)/d(GAGCCGTG) and r(CUCACGGC)/d(GCCGTGAG) hybrid duplexes at the same concentration of oligomers are shown in Fig. 3. The shapes of the melting curves of these oligomers are very similar to each other. The values of the melting temperature (T_m) are very close, 44.3 and 45.4°C, respectively. These results suggest that hybrids with identical nearest neighbors have similar melting behavior and stability.

If the melting of the RNA/DNA hybrid duplexes is a two-state transition from a double-helix state to a single-strand

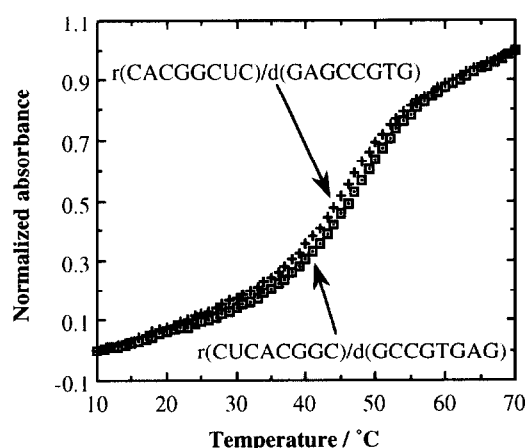


Fig. 3. Normalized melting curves of r(CACGGCUC)/d(GAGCCGTG) (+), and r(CUCACGGC)/d(GCCGTGAG) (□). The concentration of the samples was 10 μ M in 1 M NaCl-phosphate buffer.

state, the following equation can be applied in order to obtain thermodynamic parameters [12]:

$$T_m^{-1} = (2.30R/\Delta H^\circ) \log(C_t/4) + (\Delta S^\circ/\Delta H^\circ) \quad (1)$$

where T_m is the melting temperature of a duplex, ΔH° and ΔS° are enthalpy and entropy changes for duplex formation, R is the gas constant, and C_t is the total strand concentration. Plots of T_m^{-1} vs. $\log(C_t/4)$ for both hybrids are shown in Fig. 4. In Fig. 4, the plots of eq. 1 for these oligomers are very similar, and the linearity of the plots suggests the melting is due to the two-state transition, that is, double-helix to single-strand transition.

3.3. Nearest-neighbor model for RNA/DNA hybrid duplexes

Thermodynamic parameters for the duplex formation were obtained by eq. 1 in the above section and eq. 2:

$$\Delta G_{37}^\circ = \Delta H^\circ - T\Delta S^\circ \quad (2)$$

where ΔG_{37}° is the free-energy change for duplex formation at 37°C and T is 310 K. The values of ΔH° , ΔS° , and ΔG_{37}° obtained from the plots of T_m^{-1} vs. $\log(C_t/4)$, like Fig. 4, are listed in Table 1 with those of T_m for eight pairs of the RNA/DNA hybrid duplexes (16 hybrids) with identical nearest neighbors but different sequences; [A] r(GAGCCGUG)/d(CACGGCTC) and r(GCCGUGAG)/d(CTCACGGC), [B] r(CACGGCUC)/d(GAGCCGTG) and r(CUCACGGC)/d(GCCGTGAG), [C] r(AAGCGUAG)/d(CTACGCTT) and r(AGCGUAAG)/d(CTTACGCT), [D] r(ACCGCA)/d(TGCCGT) and r(GCACCG)/d(CGGTGC), [E] r(CACGGC)/d(GCCGTG) and r(GGCACG)/d(CGTGCC), [F] r(AGUCUGA)/d(TCAGGACT) and r(CUGAGUCC)/d(GGACTCAG), [G] r(CUACGCUU)/d(AAGCGTAG) and r(CUUACGCU)/d(AGCGTAAG), and [H] r(AAUGGAUUACAA)/d(TTGTAATCCATT) and r(AUUGGAUACAAA)/d(TTTGTATCCAAT). Also listed in Table 1 are the thermodynamic values for two pairs of RNA/DNA hybrid duplexes (four hybrids) with identical sequences between RNA and DNA strands but different nearest neighbors; [I] r(AGCUUCA)/d(TGAAGCT) and r(UGAAGCU)/d(AGCTTCA), and [J] r(AAUGGAUUACAA)/d(TTGTAATCCATT) contained also in pair [H] and r(UUGUAUCCAUU)/d(AATGGATTA-

CAA). Neither pair of the hybrid duplexes in pairs [I] and [J] consist of identical nearest neighbors; for example, in the case of pair [I],

$$\begin{aligned} & \text{r(AGCUUCA)/d(TGAAGCT)} \\ &= \text{rAG/dCT} + \text{rGC/dGC} + \text{rCU/dAG} + \text{rUU/dAA} + \text{rUC/dGA} + \text{rCA/dTG} \\ &\neq \text{rUG/dCA} + \text{rGA/dTC} + \text{rAA/dUU} + \text{rAG/dCT} + \text{rGC/dGC} + \text{rCU/dAG} \\ &= \text{r(UGAAGCU)/d(AGCTTCA)}. \end{aligned}$$

The nearest-neighbor model, in which the effect of the nearest-neighbor base-pair is very important for determining duplex stability, is confirmed to be reasonable for most DNA/DNA and RNA/RNA double helices [7,8]. The nearest-neighbor hypothesis predicts the pairs with identical nearest neighbors will have identical melting behaviors and identical thermodynamic parameters for duplex formation. The values of ΔH° , ΔS° , ΔG_{37}° and T_m for each duplex in pair [A] in Table 1 differ by only 1.1%, 2.0%, 3.0%, and 1.5°C, respectively. For the other pairs in Table 1, the average differences in ΔH° , ΔS° , ΔG_{37}° and T_m are 3.9%, 4.5%, 4.1%, and 1.7°C, respectively, and they are within experimental errors. In contrast, for each duplex in pairs [I] and [J] with identical sequences but different nearest neighbors, the average differences in ΔH° , ΔS° , ΔG_{37}° and T_m are 22.1%, 26.1%, 31.8%, and 11.4°C, respectively, and they are much larger than those in pairs [A]–[H]. These results indicate that the nearest-neighbor model is valid for RNA/DNA hybrid duplexes as well as RNA/RNA and DNA/DNA duplexes.

3.4. Comparison between measured and predicted

thermodynamic stabilities for RNA/DNA hybrid formation

Nearest-neighbor parameters for predicting the stability of RNA double helices were reported by Freier et al. [8]. As the structures of the RNA/DNA hybrids with identical nearest neighbors were in the A-form-like conformation as in RNA/RNA duplexes described above, we examined whether the parameters can reproduce the measured ΔG_{37}° values for the RNA/DNA hybrids in Table 1. To our knowledge, almost no promising nearest-neighbor parameters of free energy change had been determined previously for RNA/DNA hybrid duplex formation except von Hippel's parameters [3]. Unfortunately, in obtaining his parameters many hypotheses had to be used

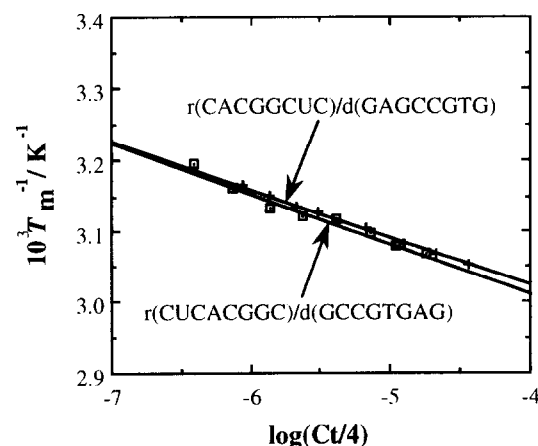


Fig. 4. Van't Hoff plots of r(CACGGCUC)/d(GAGCCGTG) (+), and r(CUCACGGC)/d(GCCGTGAG) (□). Measurements were done in 1 M NaCl-phosphate buffer at different oligomer concentrations.

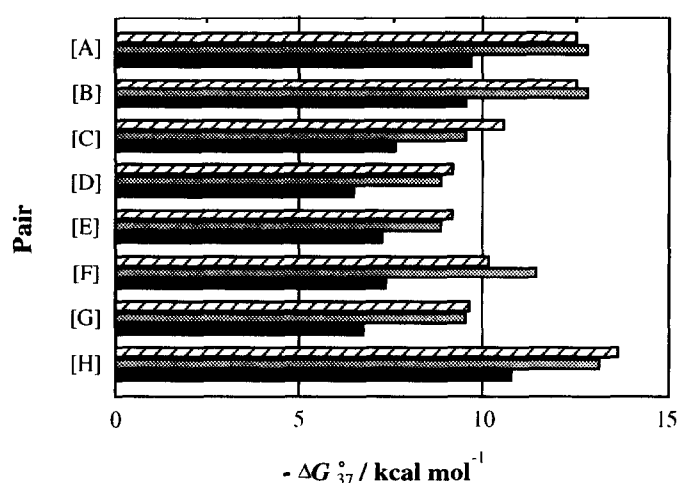


Fig. 5. Comparison of free energy changes for hybrid duplex formation measured in the present study (filled bars), and predicted with Freier's (stippled bars) and von Hippel's nearest-neighbor parameters (hatched bars). The free energy changes were calculated as average values of the oligomers with identical nearest-neighbor sequence pairs listed in Table 1.

because there were not enough experimental data about the stability to determine exactly hybrid parameters at that time. For example, the values for some nearest-neighbor sequences had to be calculated as an average of DNA/DNA parameters [7] and RNA/RNA parameters [8]. As several nearest-neighbor pairs had to be regarded as possessing the same free energy change, his parameters were given for 11 nearest-neighbor sequences, although the different parameters were necessary for 16 nearest-neighbor sequences. We also applied the parameters of von Hippel et al. to predict the measured ΔG°_{37} values for the RNA/DNA hybrids in Table 1. The results are shown in Fig. 5.

Comparing the measured ΔG°_{37} values for the hybrids with the predicted values from Freier's and von Hippel's nearest-

neighbor parameters, the average differences are 16% and 18%, respectively. The largest difference is 34% for the RNA/RNA parameters and 24% for the RNA/DNA ones. These differences are significantly larger than that expected. Therefore, it is suggested that the nearest-neighbor model is valid in RNA/DNA duplexes as well as RNA/RNA and DNA/DNA ones, but the thermodynamic parameters for the nearest neighbors should be improved or newly determined in order to predict more precisely the stability of RNA/DNA hybrid duplexes.

Acknowledgements: This work was supported in part by grants from the Ministry of Education, Science and Culture, Japan, Hyogo Science and Technology Association, Inamori Foundation, and Hirao Science Foundation (to N.S.).

References

- [1] von Hippel, P.H., Bear, D.G., Morgan, W.D. and McSwinggen, J.A. (1984) *Annu. Rev. Biochem.* 53, 389–446.
- [2] Varmus, H.E. (1982) *Science* 216, 812–820.
- [3] Yager, T.D. and von Hippel, P.H. (1991) *Biochemistry* 30, 1097–1118.
- [4] Stein, C.A. and Cheng, Y.-C. (1993) *Science* 261, 1004–1012.
- [5] Blake, K.R., Murakami, A. and Miller, P.S. (1985) *Biochemistry* 24, 6132–6138.
- [6] Shimayama, T., Nishikawa, F., Nishikawa, S. and Taira, K. (1993) *Nucleic Acids Res.* 21, 2605–2611.
- [7] Breslauer, K.J., Frank, R., Blöcker, H. and Marky, L.A. (1986) *Proc. Natl. Acad. Sci. USA* 83, 3746–3750.
- [8] Freier, S.M., Kierzek, R., Jaeger, J.A., Sugimoto, N., Caruthers, M.H., Neilson, T. and Turner, D.H. (1986) *Proc. Natl. Acad. Sci. USA* 83, 9373–9377.
- [9] Sugimoto, N., Kierzek, R., Freier, S.M. and Turner, D.H. (1986) *Biochemistry* 25, 5755–5759.
- [10] Sugimoto, N., Kierzek, R. and Turner, D.H. (1987) *Biochemistry* 26, 4554–4558.
- [11] Sugimoto, N., Kierzek, R. and Turner, D.H. (1987) *Biochemistry* 26, 4559–4562.
- [12] Turner, D.H., Sugimoto, N. and Freier, S.M. (1990) *Landolt-Bornstein: Nucleic Acids*, vol. 1c (Saenger, W.R., ed.) ch. 3.6.
- [13] Longfellow, C.E., Kierzek, R. and Turner, D.H. (1990) *Biochemistry* 29, 278–285.

Table 1
Thermodynamic parameters for hybrid formation*

Pair	Hybrid duplex	ΔH° (kcal · mol ⁻¹)	ΔS° (cal · mol ⁻¹ · K ⁻¹)	ΔG°_{37} (kcal · mol ⁻¹)	T_m^{**} (°C)
[A]	r(GAGCCGUG)/d(CACGGCTC)	-67.2	-186	-9.6	51.9
	r(GCCGUGAG)/d(CTCACGGC)	-69.1	-192	-9.7	51.8
[B]	r(CACGGCUC)/d(GAGCCGTG)	-69.0	-193	-9.1	48.8
	r(CUCACGGC)/d(GCCGTGAG)	-68.0	-187	-9.9	53.1
[C]	r(AAGCGUAG)/d(CTACGCTT)	-66.6	-190	-7.7	42.7
	r(AGCGUAAG)/d(CTTACGCT)	-61.5	-174	-7.5	42.1
[D]	r(ACCGCA)/d(TGCGGT)	-45.4	-126	-6.5	36.6
	r(GCACCG)/d(CG GTGC)	-47.9	-134	-6.4	36.3
[E]	r(CACGGC)/d(GCCGTG)	-47.3	-129	-7.1	40.5
	r(GGCACG)/d(CG TGCC)	-50.0	-138	-7.3	41.6
[F]	r(AGUCCUGA)/d(TCAGGACT)	-55.7	-158	-6.8	38.7
	r(CUGAGUCC)/d(GGACTCAG)	-59.0	-165	-7.8	43.8
[G]	r(CUACGCUU)/d(AAGCGTAG)	-52.1	-146	-6.8	38.9
	r(CUUACGCU)/d(AGCGTAAG)	-52.7	-149	-6.6	37.4
[H]	r(AAUGGAUUACAA)/d(TTGTAATCCATT)	-94.1	-269	-10.7	51.4
	r(AUUGGAUACAAA)/d(TTTGTATCCAAT)	-92.9	-265	-10.7	51.8
[I]	r(AGCUUCA)/d(TGAAGCT)	-54.1	-159	-4.8	25.1
	r(UGAAGCU)/d(AGCTTCA)	-41.8	-112	-6.9	40.0
[J]	r(AAUGGAUUACAA)/d(TTGTAATCCATT)	-94.1	-269	-10.7	51.4
	r(UUGUAAUCCA UU)/d(AATGGATTACAA)	-78.2	-226	-8.1	43.6

*All experiments were done in a buffer of 1 M NaCl 10 mM Na₂HPO₄ 1 mM Na₂EDTA, pH 7.0.

**Melting temperatures are calculated at the total oligomer concentration of 100 μM.

- [14] Peritz, A.E., Kierzek, R., Sugimoto, N. and Turner, D.H. (1991) *Biochemistry* 30, 6428–6436.
- [15] Sugimoto, N. and Sasaki, M. (1991) *Chem. Lett.* 345–348.
- [16] Sugimoto, N., Matumura, A. and Sasaki, M. (1993) *Chem. Express* 8, 309–312.
- [17] Pyle, A.M., Murphy, F.L. and Cech, T.R. (1992) *Nature* 358, 123–128.
- [18] LeCuyer, K.A. and Crothers, D.M. (1993) *Biochemistry* 32, 5301–5311.
- [19] Connell, G.J. and Yayus, M. (1994) *Science* 264, 1137–1141.
- [20] Richards, E.G. (1975) *Handbook of Biochemistry and Molecular Biology; Nucleic Acids*, vol. 1 (Fasman, G.D., ed.) pp. 597, 3rd edn., CRC Press.
- [21] Sugimoto, N., Tanaka, A., Shintani, Y. and Sasaki, M. (1991) *Chem. Lett.* 9–12.
- [22] Sugimoto, N., Shintani, Y., Tanaka, A. and Sasaki, M. (1992) *Bull. Chem. Soc. Jpn.* 65, 535–540.
- [23] Borer, P.N., Dengler, B., Tinoco Jr., I. and Uhlenbeck, O.C. (1974) *J. Mol. Biol.* 86, 843–853.
- [24] Saenger, W.R. (1984) *Principles of Nucleic Acid Structure*, Springer-Verlag.
- [25] Williamson, J.R., Raghuraman, M.K. and Cech, T.R. (1989) *Cell* 59, 871–880.